

52. Naya, M.; Kobayashi, N.; Mizuno, K.; Matsumoto, K.; Ema, M.; Nakanishi, J. Evaluation of the genotoxic potential of single-wall carbon nanotubes by using a battery of *in vitro* and *in vivo* genotoxicity assays. *Regul. Toxicol. Pharmacol.* **2011**, *61*, 192–198.
53. Magrez, A.; Kasas, S.; Salicio, V.; Pasquier, N.; Seo, J.W.; Celio, M.; Catsicas, S.; Schwaller, B.; Forro, L. Cellular toxicity of carbon-based nanomaterials. *Nano Lett.* **2006**, *6*, 1121–1125.
54. Jacobsen, N.R.; Pojana, G.; White, P.; Moller, P.; Cohn, C.A.; Korsholm, K.S.; Vogel, U.; Marcomini, A.; Loft, S.; Wallin, H. Genotoxicity, cytotoxicity, and reactive oxygen species induced by single-walled carbon nanotubes and C(60) fullerenes in the FE1-Muttrade mark Mouse lung epithelial cells. *Environ. Mol. Mutagen.* **2008**, *49*, 476–487.
55. Di Sotto, A.; Chiaretti, M.; Carru, G.A.; Bellucci, S.; Mazzanti, G. Multi-walled carbon nanotubes: Lack of mutagenic activity in the bacterial reverse mutation assay. *Toxicol. Lett.* **2009**, *184*, 192–197.
56. Nagai, H.; Okazaki, Y.; Chew, S.H.; Misawa, N.; Yamashita, Y.; Akatsuka, S.; Ishihara, T.; Yamashita, K.; Yoshikawa, Y.; Yasui, H.; *et al.* Diameter and rigidity of multiwalled carbon nanotubes are critical factors in mesothelial injury and carcinogenesis. *Proc. Natl. Acad. Sci. USA* **2011**, *108*, E1330–E1338.
57. Shvedova, A.A.; Kisin, E.; Murray, A.R.; Johnson, V.J.; Gorelik, O.; Arepalli, S.; Hubbs, A.F.; Mercer, R.R.; Keohavong, P.; Sussman, N.; *et al.* Inhalation vs. aspiration of single-walled carbon nanotubes in C57BL/6 mice: Inflammation, fibrosis, oxidative stress, and mutagenesis. *Am. J. Physiol. Lung Cell. Mol. Physiol.* **2008**, *295*, L552–L565.
58. Shvedova, A.A.; Kisin, E.R.; Mercer, R.; Murray, A.R.; Johnson, V.J.; Potapovich, A.I.; Tyurina, Y.Y.; Gorelik, O.; Arepalli, S.; Schwegler-Berry, D.; *et al.* Unusual inflammatory and fibrogenic pulmonary responses to single-walled carbon nanotubes in mice. *Am. J. Physiol. Lung Cell. Mol. Physiol.* **2005**, *289*, L698–L708.
59. Johnston, H.J.; Hutchison, G.R.; Christensen, F.M.; Peters, S.; Hankin, S.; Aschberger, K.; Stone, V. A critical review of the biological mechanisms underlying the *in vivo* and *in vitro* toxicity of carbon nanotubes: The contribution of physico-chemical characteristics. *Nanotoxicology* **2010**, *4*, 207–246.
60. Donaldson, K.; Murphy, F.; Schinwald, A.; Duffin, R.; Poland, C.A. Identifying the pulmonary hazard of high aspect ratio nanoparticles to enable their safety-by-design. *Nanomedicine* **2011**, *6*, 143–156.
61. Donaldson, K.; Murphy, F.A.; Duffin, R.; Poland, C.A. Asbestos, carbon nanotubes and the pleural mesothelium: A review of the hypothesis regarding the role of long fibre retention in the parietal pleura, inflammation and mesothelioma. *Part. Fibre Toxicol.* **2010**, *7*, 5.
62. Migliore, L.; Saracino, D.; Bonelli, A.; Colognato, R.; D’Errico, M.R.; Magrini, A.; Bergamaschi, A.; Bergamaschi, E. Carbon nanotubes induce oxidative DNA damage in RAW 264.7 cells. *Environ. Mol. Mutagen.* **2010**, *51*, 294–303.
63. Vittorio, O.; Raffa, V.; Cuschieri, A. Influence of purity and surface oxidation on cytotoxicity of multiwalled carbon nanotubes with human neuroblastoma cells. *Nanomedicine* **2009**, *5*, 424–431.
64. Dostert, C.; Petrilli, V.; Van Bruggen, R.; Steele, C.; Mossman, B.T.; Tschopp, J. Innate immune activation through Nalp3 inflammasome sensing of asbestos and silica. *Science* **2008**, *320*, 674–677.

65. Palomaki, J.; Valimaki, E.; Sund, J.; Vippola, M.; Clausen, P.A.; Jensen, K.A.; Savolainen, K.; Matikainen, S.; Alenius, H. Long, needle-like carbon nanotubes and asbestos activate the NLRP3 inflammasome through a similar mechanism. *ACS Nano* **2011**, *5*, 6861–6870.
66. Yang, S.T.; Wang, X.; Jia, G.; Gu, Y.; Wang, T.; Nie, H.; Ge, C.; Wang, H.; Liu, Y. Long-term accumulation and low toxicity of single-walled carbon nanotubes in intravenously exposed mice. *Toxicol. Lett.* **2008**, *181*, 182–189.
67. Wick, P.; Manser, P.; Limbach, L.K.; Dettlaff-Weglikowska, U.; Krumeich, F.; Roth, S.; Stark, W.J.; Bruinink, A. The degree and kind of agglomeration affect carbon nanotube cytotoxicity. *Toxicol. Lett.* **2007**, *168*, 121–131.
68. Murray, A.R.; Kisin, E.; Leonard, S.S.; Young, S.H.; Kommineni, C.; Kagan, V.E.; Castranova, V.; Shvedova, A.A. Oxidative stress and inflammatory response in dermal toxicity of single-walled carbon nanotubes. *Toxicology* **2009**, *257*, 161–171.
69. Aschberger, K.; Johnston, H.J.; Stone, V.; Aitken, R.J.; Hankin, S.M.; Peters, S.A.; Tran, C.L.; Christensen, F.M. Review of carbon nanotubes toxicity and exposure—Appraisal of human health risk assessment based on open literature. *Crit. Rev. Toxicol.* **2010**, *40*, 759–790.
70. Ai, J.; Biazar, E.; Jafarpour, M.; Montazeri, M.; Majdi, A.; Aminifard, S.; Zafari, M.; Akbari, H.R.; Rad, H.G. Nanotoxicology and nanoparticle safety in biomedical designs. *Int. J. Nanomed.* **2011**, *6*, 1117–1127.
71. Stefani, D.; Paula, A.J.; Vaz, B.G.; Silva, R.A.; Andrade, N.F.; Justo, G.Z.; Ferreira, C.V.; Filho, A.G.; Eberlin, M.N.; Alves, O.L. Structural and proactive safety aspects of oxidation debris from multiwalled carbon nanotubes. *J. Hazard Mater.* **2011**, *189*, 391–396.
72. Rourke, J.P.; Pandey, P.A.; Moore, J.J.; Bates, M.; Kinloch, I.A.; Young, R.J.; Wilson, N.R. The real graphene oxide revealed: Stripping the oxidative debris from the graphene-like sheets. *Angew. Chem. Int. Ed. Engl.* **2011**, *50*, 3173–3177.
73. Fogden, S.; Verdejo, R.; Cottam, B.; Shaffer, M. Purification of single walled carbon nanotubes: The problem with oxidation debris. *Chem. Phys. Lett.* **2008**, *460*, 162–167.
74. Ryman-Rasmussen, J.P.; Cesta, M.F.; Brody, A.R.; Shipley-Phillips, J.K.; Everitt, J.I.; Tewksbury, E.W.; Moss, O.R.; Wong, B.A.; Dodd, D.E.; Andersen, M.E.; *et al.* Inhaled carbon nanotubes reach the subpleural tissue in mice. *Nat. Nanotechnol.* **2009**, *4*, 747–751.
75. Kagan, V.E.; Konduru, N.V.; Feng, W.; Allen, B.L.; Conroy, J.; Volkov, Y.; Vlasova, I.I.; Belikova, N.A.; Yanamala, N.; Kapralov, A.; *et al.* Carbon nanotubes degraded by neutrophil myeloperoxidase induce less pulmonary inflammation. *Nat. Nanotechnol.* **2010**, *5*, 354–359.
76. Liu, X.; Hurt, R.H.; Kane, A.B. Biodurability of single-walled carbon nanotubes depends on surface functionalization. *Carbon* **2010**, *48*, 1961–1969.
77. Yamashita, K.; Yoshioka, Y.; Higashisaka, K.; Morishita, Y.; Yoshida, T.; Fujimura, M.; Kayamuro, H.; Nabeshi, H.; Yamashita, T.; Nagano, K.; *et al.* Carbon nanotubes elicit DNA damage and inflammatory response relative to their size and shape. *Inflammation* **2010**, *33*, 276–280.
78. Coccini, T.; Roda, E.; Sarigiannis, D.A.; Mustarelli, P.; Quartarone, E.; Profumo, A.; Manzo, L. Effects of water-soluble functionalized multi-walled carbon nanotubes examined by different cytotoxicity methods in human astrocyte D384 and lung A549 cells. *Toxicology* **2010**, *269*, 41–53.

79. Nabeshi, H.; Yoshikawa, T.; Matsuyama, K.; Nakazato, Y.; Matsuo, K.; Arimori, A.; Isobe, M.; Tochigi, S.; Kondoh, S.; Hirai, T.; *et al.* Systemic distribution, nuclear entry and cytotoxicity of amorphous nanosilica following topical application. *Biomaterials* **2011**, *32*, 2713–2724.
80. Nabeshi, H.; Yoshikawa, T.; Matsuyama, K.; Nakazato, Y.; Tochigi, S.; Kondoh, S.; Hirai, T.; Akase, T.; Nagano, K.; Abe, Y.; *et al.* Amorphous nanosilica induce endocytosis-dependent ROS generation and DNA damage in human keratinocytes. *Part. Fibre Toxicol.* **2011**, *8*, 1.
81. Nabeshi, H.; Yoshikawa, T.; Arimori, A.; Yoshida, T.; Tochigi, S.; Hirai, T.; Akase, T.; Nagano, K.; Abe, Y.; Kamada, H.; *et al.* Effect of surface properties of silica nanoparticles on their cytotoxicity and cellular distribution in murine macrophages. *Nanoscale Res. Lett.* **2011**, *6*, 93.
82. Lundqvist, M.; Stigler, J.; Elia, G.; Lynch, I.; Cedervall, T.; Dawson, K.A. Nanoparticle size and surface properties determine the protein corona with possible implications for biological impacts. *Proc. Natl. Acad. Sci. USA* **2008**, *105*, 14265–14270.
83. Sund, J.; Alenius, H.; Vippola, M.; Savolainen, K.; Puustinen, A. Proteomic characterization of engineered nanomaterial-protein interactions in relation to surface reactivity. *ACS Nano* **2011**, *5*, 4300–4309.
84. Gasser, M.; Rothen-Rutishauser, B.; Krug, H.F.; Gehr, P.; Nelle, M.; Yan, B.; Wick, P. The adsorption of biomolecules to multi-walled carbon nanotubes is influenced by both pulmonary surfactant lipids and surface chemistry. *J. Nanobiotechnol.* **2010**, *8*, 31.
85. Moghimi, S.M.; Hunter, A.C. Complement monitoring of carbon nanotubes. *Nat. Nanotechnol.* **2010**, *5*, 382.

© 2012 by the authors; licensee MDPI, Basel, Switzerland. This article is an open access article distributed under the terms and conditions of the Creative Commons Attribution license (<http://creativecommons.org/licenses/by/3.0/>).

4 ナノカーボン DDS の現状とその安全性確保に向けて

4.1 はじめに 平井敏郎*¹, 吉岡靖雄*², 鍋師裕美*³, 吉川友章*⁴, 堤 康央*⁵

少なくとも1次元が100nm以下の大きさであるナノマテリアル (NM) は、サブミクロンサイズ以上 (100nm以上) の従来素材とは異なる画期的機能を発揮することから、様々な分野で夢の新素材として期待されている。特に医療分野では、高い組織浸透性や、薬物保持・徐放化能を利用して、低分子化合物やタンパク質単独では期待できなかった薬効を示す画期的新薬 (ナノメディシン) の開発が世界中で進められている。これら NM の画期的機能は、ナノ医薬としての主薬あるいはナノ添加剤としてだけでなく、“薬物を必要なときに、必要な量、必要な所へ到達させることで、副作用を最小限に抑え、最大の効果を発揮させる” という理想の投薬形態、薬物治療の最適化を目指したドラッグデリバリーシステム (DDS) そのものであり、まさに、ナノメディシン=ナノ DDS と言えよう。周知のように、DDS 研究領域へのナノテクノロジー・ナノマテリアルの導入はファミリアとなりつつあり、例えば、100nm以下のサイズに厳密制御したリポソームやナノスフェア、 dendrimer の開発が果敢に試みられている。一方で、これらナノメディシンの開発はまだ緒に就いたばかりであり、多くは未だブラックボックスと言え、その魅力的で秘められた可能性が逆に、予想外の部位で未知の副作用を発現させる潜在的な脅威にもなっている。しかし、現行の NM の安全性研究の大部分はハザード同定 (副作用の有無の評価) のみに偏重しており、NM の物性と体内吸収性や体内/細胞内動態、生体影響の連関といった、NM の安全性担保に資する具体的な情報が圧倒的に不足している。このままでは、全ての NM の安全性に対する懸念が広がり、ナノメディシン開発の足枷になりかねない。従って、NM を用いたナノメディシンの開発を実現・推進するためには、副作用を含めた生体影響を詳細に解析したうえで、それらの情報を基盤として有効かつ安全な NM の開発を推進するほか無い。即ち、単にナノマテリアルのハザード (毒性) やリスク (危険性)、そのメカニズム (毒性発現機

*1 Toshiro Hirai 大阪大学 大学院薬学研究科 毒性学分野; (株)医薬基盤研究所 バイオ創薬プロジェクト

*2 Yasuo Yoshioka 大阪大学 臨床医工学融合研究教育センター 特任准教授 (常勤); (株)医薬基盤研究所 バイオ創薬プロジェクト

*3 Hiromi Nabeshi 大阪大学 大学院薬学研究科 附属実践薬学教育研究センター 特任助教 (常勤); (株)医薬基盤研究所 バイオ創薬プロジェクト

*4 Tomoaki Yoshikawa 大阪大学 大学院薬学研究科 毒性学分野 助教; (株)医薬基盤研究所 バイオ創薬プロジェクト

*5 Yasuo Tsutsumi 大阪大学 大学院薬学研究科 毒性学分野 教授; (株)医薬基盤研究所 バイオ創薬プロジェクト; 大阪大学 臨床医工学融合研究教育センター

構)を解明しようとするナノ毒性学(Nano-Toxicology)では、現状を打破できないであろう。むしろ、ヒトと生態系(環境)にとって安全で、ヒトと社会(産業界など)がナノテクノロジーの恩恵を最大限に享受でき、しかも安心して豊かな生活を営めるよう、安全なナノメディシン(ナノDDS)の開発とその支援に叶うナノ安全科学研究(Nano-Safety Science)とも言うべき学問が今後の鍵となっている(図1)。NMとヒト、生態系との共存、社会受容、これらがまさにキーポイントであろう。そこで本総説では、特にDDS医薬に適した特徴的な物性を有するナノカーボン素材を例に、ナノメディシン開発の現状とともに、ナノメディシンの開発に必須であるNMの安全性確保に向けて我々が推進しているナノ安全科学研究を含めて紹介させていただきたい¹⁾。

4.2 ナノカーボンDDSの可能性

近年、フラーレン、カーボンナノチューブ(CNT)やカーボンナノホーン(CNH)など、ナノカーボン素材を用いたDDS医薬の開発が注目を浴びている。これらは、炭素間結合を介す長い電子共役系を持つなど特殊な物性を有し、高い薬物保持能や生体内安定性、柔軟な構造(表面修飾の容易さ)といった、DDS素材として極めて有望な性質を発揮する。この特性を活かし、低分子医薬、タンパク質医薬、核酸医薬の送達キャリアとしての開発が前臨床段階ではあるものの、世界中で進められている。近年では、腫瘍組織、炎症組織や細胞内リソソームなど低pH環境において薬剤が放出されるといったDDS機能を有するナノカーボン素材の開発も進められている。また、ナノカーボン素材は内腔を持つ特殊な構造を有するため、表面だけではなくその内

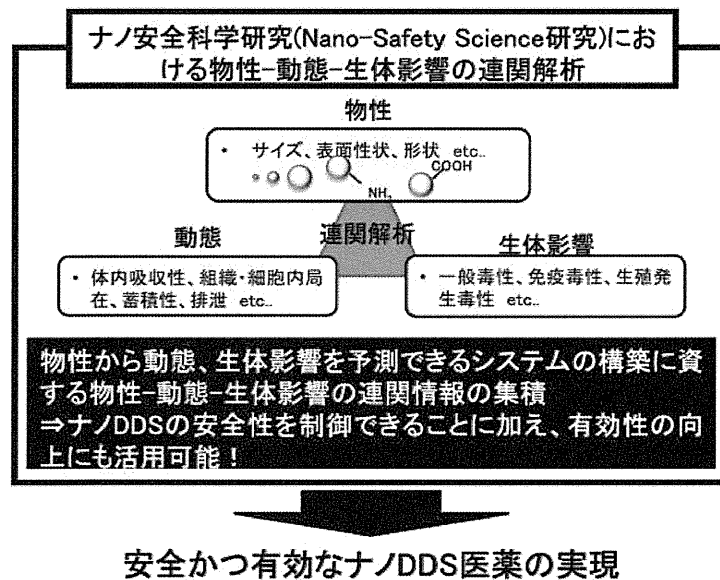


図1 ナノDDS医薬の実現に向けたナノ安全科学研究

腔に薬物を保持させ、徐放化を試みる検討もある。湯田坂らは、CNHに内包されたシスプラチンが数十時間をかけて徐放され、顕著な抗がん作用を示すことを報告している⁵⁾。さらに、薬物キャリアとしてのみならず、ナノカーボン素材自身が有する薬理活性を利用した医薬品応用にも期待が寄せられている。例えば、ナノカーボン素材特有の長い電子共役系によって誘導される光増感物質としての性質は、がんの光線力学的治療法、フォトダイナミックセラピー（PDT）に応用することが可能である。田畑らは、フラーレンへの光照射により一重項酸素などの活性酸素が非常に高い効率で発生する性質を利用し、*in vivo*において顕著な腫瘍退縮効果が得られることを報告している⁶⁾。一方でこれら電子共役系により、フラーレンはラジカルスポンジとも呼ばれるほど強い抗酸化作用を有し、活性酸素が原因となり発症・悪化する各種炎症性疾患への適用も進められている。さらに近年、神経幹細胞を用いた脳卒中の治療において、CNTを幹細胞の足場として用いることで組織修復が劇的に向上し、神経保護作用を発揮することで虚血性傷害を軽減させ得ることが明らかとなった⁷⁾。このように、ナノカーボン素材の有用機能について、続々と予期せぬ新規作用が見出されつつあり、今後も新たな治療戦略の開発に期待が寄せられている。また、ナノカーボン素材は表面修飾が容易であることから、各種リガンド・抗体を用いたターゲティング能の付加による治療効果増大・副作用低減を目指した試みも精力的になされている。さらに、現在、解析技術がボトルネックとなり不足している体内動態に関する情報の蓄積が進展すれば、ナノカーボン素材の医薬品応用に、より一層の飛躍が見込まれる。

4.3 安全なナノ DDS 医薬の開発に向けて







ナノカーボン素材のナノメディシンへの応用研究は多数なされている一方で、体内・組織内・細胞内動態や副作用情報（NanoTox）は未だ乏しいのが現状である。さらに、ナノカーボン素材を含めたNMの物性と体内動態、生体影響との関連性については、全く体系的に理解されておらず、有効かつ安全なナノメディシンの開発に資する基盤情報の収集が急務となっている。例えばナノカーボン素材に関して、CNTがアスベストと同様に悪性中皮腫や肺がんを誘発する可能性が報告される一方で⁸⁾、血中投与後、長期にわたって一切の毒性が観察されないとする報告が存在するなど⁹⁾、一見矛盾する報告が飛び交っている。しかし、これら検討に用いられているCNTは、多層、単層と構造的な差異があるとともに、太さや長さといった形状、さらには混入している不純物までもが異なっている。また、これら物性の違いに応じて変化すると考えられる動態に関しての情報も皆無であり、一部のハザード情報のみが一人歩きすることで、むやみに危険性を煽り、ひいてはその風評被害により、有益なナノカーボン素材までもを闇に葬りかねない。本観点から我々は、NMの安全性確保及び安全なNMの創製に資する基盤情報の収集を目的としたナノ安全科学研究を推進しており、NMの物性と体内動態、生体影響の連関評価を試みてきた。ここでは、我々のナノ安全科学研究の中から、遺伝子送達キャリアなどのDDS素材として期待されるナノシリカ（nSP）を用いた先行研究について紹介させていただきたい。我々はこれまでの検討から、粒子径100nm以下のnSPが、経皮・経口・経鼻等の非侵襲的な経路からの

第6章 DDSの新たな可能性

投与においても体内吸収され、脳や胎盤といった特にバリア機能の発達した部位や、細胞の核内にまで到達し得ることを明らかとしてきた³⁾。本結果は、nSPがこれまで送達不可能であった部位への薬物送達をも可能とする新規キャリアになり得ることを示すものであり、我々も核酸送達キャリアやワクチンキャリアとしての適用を試み、興味深い知見を得つつある。そこで、粒子径70nmのnSP (nSP70) と、対照群として300, 1000nmの従来型シリカ (nSP300, mSP1000) を用い、粒子径と体内局在、ハザードとの関係を精査した。まず、体内吸収後の安全性評価の観点から、静脈内投与後の各粒子の局在を、*in vivo* イメージングにより解析した。その結果、6時間後にはnSP300, mSP1000が胆のうにのみ集積していたのに対し、nSP70は肝臓全体に広がって分布していることが示された。さらに、透過型電子顕微鏡観察の結果、nSP70のみが肝実質細胞内にまで侵入しており、この結果と相関して、過剰量の投与では、nSP70投与群でのみ肝実質細胞の強い傷害に起因した重篤な肝障害や、血液凝固系異常などを伴う急性致死毒性が観察された。また、これら劇的なハザードが観察されない投与量においても、nSP70の妊娠母体への投与によって、nSP70のみが胎盤に移行し、さらには血液胎盤関門を突破して胎仔にまで侵入することから、胎仔発育不全の誘発に注意する必要があることを明らかとした⁴⁾。以上の結果から、粒子径の違いにより、シリカの体内・細胞内動態、さらにはその生体影響までもが変化することが示された。次に、安全なnSPの創製に向け、nSP70の表面がアミノ基、カルボキシル基で修飾されたnSP70-N, nSP70-Cを用いて、表面性状と生体影響の関係を精査した。その結果、表面修飾体ではnSP70で認められた急性致死毒性や胎仔毒性等が一切観察されず、安全性が飛躍的に向上することが明らかとなった^{2,4)}。すなわち、本研究の最も重要な点は、nSPの表面修飾が、その有効性を保持しつつ、安全性を担保できる極めて有望なアプローチになり得る可能性が示されたことである。以上のnSPでの先行研究を受け、現在、ナノカーボン素材に関しても、物性と動態、生体影響の関連情報を収集している。一例をあげると、これまでに我々は、様々な物性のCNTを用い、CNTによるDNA傷害性や起炎性といったハザードが、長さ、太さといったCNTの形状(物性)により規定され、長さとおさを各々1-2 μ m以下、10nm以下程度に制御することで、安全性が向上する可能性を明らかとしている¹⁾(図2)。また、フラーレンは適切な表面修飾により、高度に安全性を確保しつつ、圧倒的な抗炎症作用を発揮させ得ることを我々は認めており、現在、その実用化を目指した研究を推進中である。今後は、ナノカーボン素材に関しても、表面修飾による表面性状の変化と、生体影響との関連解明を図ることで、より安全性に優れた素材の創製が可能になると期待される。

4.4 おわりに

本総説では、ナノカーボン素材によるナノメディシンの実現に向け、ナノDDSへの適用の現状とともに、最も急がれる安全性確保に関する検討を中心に紹介させていただいた。これまでのナノDDS医薬開発において、その安全性が懸念されていたことの根底には、従来の化審法と同様、物質名のみに基づいた安全性の議論が中核であったことも一因にある。裏を返せばこれは、

種類	 M1 多層CNT	 M2 多層CNT	 M3 多層CNT
直径	5-15 μm	1-2 μm	1-2 μm
長さ	20-60 nm	60-100 nm	< 10 nm
安全性 (DNA傷害性、in vivo起 炎性を指標として)			

Ref. Yamashita, K. *et al.*, *Inflammation*, 33 (4): 276-80 (2010)

図2 カーボンナノチューブの物性と安全性の関連情報

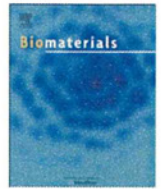
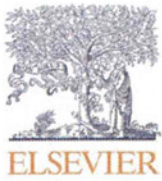
NMの物性と、動態やハザードとの関連情報などの、NMの安全性確保に資する具体的情報が圧倒的に不足していたことを意味している。今回、表面性状や形状など物性の適切な制御により、安全性を高めうることを紹介したが、未だ基礎情報は不足しており、引き続きナノ安全科学研究を推進していくこと、そして何よりDDS研究との高度な有機的融合が必要不可欠である。また、物性制御により、NMの安全性が高度に担保されるメカニズムの解明が今後の課題であると考えられ、メカニズムに関する議論を深めることで、他のNMにも適用可能なより普遍性を持った安全性情報を蓄積することが可能になると期待される。末筆ではあるが、最も重要なことは、最適条件でのNM創出により、安全なNMを創出できること、安全なNMは圧倒的な知財であり、ヒトの健康確保と、責任ある先進国・技術立国として、健康立国として我が国の発展に大いに貢献し得ることである。言い換えれば、『新たに産み出されるDDS医薬（ナノメディンを含む）が有効なのは当たり前で、さらに高度な安全性を保障していく』ことの重要度は、ますます加速していこう。今後、ナノメディンやナノDDSの開発と実用化に向け、ナノ開発研究とナノ安全科学研究が強固に連携し、両輪となって共に歩むことで、ナノDDS開発が飛躍的に進歩することを祈念してやまない。

文 献

- 1) Yamashita, K. *et al.*, *Inflammation*, 33 (4), 276-80 (2010)

第6章 DDSの新たな可能性

- 2) Nabeshi H. *et al.*, *Nanoscale Research Letters*, **6** (1), 93 (2011)
- 3) Nabeshi, H. *et al.*, *Biomaterials*, **32** (11), 2713–24 (2011)
- 4) Yamashita, K. *et al.*, *Nat. Nanotechnol.*, **6** (5), 321–8 (2011)
- 5) Ajima, K. *et al.*, *Mol. Pharm.*, **2**, 475–80 (2005)
- 6) Tabata, Y. *et al.*, *Fullerene Sci. Technol.*, **5**, 989–1007 (1987)
- 7) Lee, HJ. *et al.*, *Nat. Nanotech.*, **6**, 121–5 (2011)
- 8) Poland, CA. *et al.*, *Nat. Nanotech.*, **3**, 423–28 (2008)
- 9) Schipper, ML. *et al.*, *Nat. Nanotech.*, **3**, 216–21 (2008)



Leading Opinion

Acute phase proteins as biomarkers for predicting the exposure and toxicity of nanomaterials[☆]

Kazuma Higashisaka^{a,b,1}, Yasuo Yoshioka^{a,b,c,*}, Kohei Yamashita^{a,b}, Yuki Morishita^{a,b}, Maho Fujimura^{a,b}, Hiromi Nabeshi^a, Kazuya Nagano^b, Yasuhiro Abe^b, Haruhiko Kamada^{b,c}, Shin-ichi Tsunoda^{b,c,d}, Tomoaki Yoshikawa^{a,b}, Norio Itoh^a, Yasuo Tsutsumi^{a,b,c,**}

^a Department of Toxicology and Safety Science, Graduate School of Pharmaceutical Sciences, Osaka University, 1-6 Yamadaoka, Suita, Osaka 565-0871, Japan

^b Laboratory of Pharmaceutical Proteomics, National Institute of Biomedical Innovation, 7-6-8, Saito-Asagi, Ibaraki, Osaka 567-0085, Japan

^c The Center for Advanced Medical Engineering and Informatics, Osaka University, 1-6, Yamadaoka, Suita, Osaka 565-0871, Japan

^d Department of Biomedical Innovation, Graduate School of Pharmaceutical Sciences, Osaka University, 7-6-8, Saito-Asagi, Ibaraki, Osaka 567-0085, Japan

ARTICLE INFO

Article history:

Received 8 July 2010

Accepted 31 August 2010

Available online 22 September 2010

Keywords:

Nanoparticle

Plasma proteins

Silica

Surface modification

ABSTRACT

Recently, nanomaterials have become an integral part of our daily lives. However, there is increasing concern about the potential risk to human health. Here, we attempted to identify biomarkers for predicting the exposure and toxicity of nanomaterials by using a proteomics based approach. We evaluated the changes of protein expression in plasma after treatment with silica nanoparticles. Our analyses identified haptoglobin, one of the acute phase proteins, as a candidate biomarker. The results of ELISA showed that the level of haptoglobin was significantly elevated in plasma of mice exposed to silica nanoparticles with a diameter of 70 nm (nSP70) compared to normal mice and those exposed to silica particles with a diameter of 1000 nm. Furthermore, the other acute phase proteins, C-reactive protein (CRP) and serum amyloid A (SAA) were also elevated in plasma of nSP70 treated mice. In addition, the level of these acute phase proteins was elevated in the plasma of mice after intranasal treatment with nSP30. Our results suggest that haptoglobin, CRP and SAA are highly sensitive biomarkers for assessing the risk of exposure to silica nanoparticles. We believe this study will contribute to the development of global risk assessment techniques for nanomaterials.

© 2010 Elsevier Ltd. All rights reserved.

1. Introduction

With the recent development of nanotechnology, nanomaterials such as silica nanoparticles are beginning to be used on a global scale. In comparison to conventional materials with submicron size, nanomaterials display unique properties such as high levels of

electrical conductivity, tensile strength and chemical reactivity [1]. Nanomaterials have already been used in various fields such as electronic engineering, cosmetics and medicine [2,3]. Because nanotechnology is emerging as a leading industrial sector, humans will be increasingly exposed to a wide range of synthetic nanomaterials with diverse properties.

The increasing use of nanomaterials has raised public concerns about the potential risks to human health [4–6]. For example, it is reported that carbon nanotubes induce mesothelioma-like lesions in mice in a similar way to crocidolite asbestos [7]. Other reports showed that exposure to titanium dioxide particles induce inflammatory responses and lung injury in mice [8,9]. In addition, our group showed that silica nanoparticles with a diameter of 70 nm can penetrate mouse skin and enter the circulatory system (unpublished data). Furthermore our group demonstrated that silica nanoparticles induce severe liver damage after systemic administration [10–12]. However, current knowledge of the potential risk of nanomaterials is considered insufficient. Indeed, concerns about the potential dangers of nanomaterials have led the World Health Organization and the Organization for Economic

[☆] *Editor's Note:* This paper is one of a newly instituted series of scientific articles that provide evidence-based scientific opinions on topical and important issues in biomaterials science. They have some features of an invited editorial but are based on scientific facts, and some features of a review paper, without attempting to be comprehensive. These papers have been commissioned by the Editor-in-Chief and reviewed for factual, scientific content by referees.

* Corresponding author. The Center for Advanced Medical Engineering and Informatics, Osaka University, 1-6 Yamadaoka, Suita, Osaka 565-0871, Japan. Tel.: +81 6 6879 8230; fax: +81 6 6879 8234.

** Corresponding author. Department of Toxicology and Safety Science, Graduate School of Pharmaceutical Sciences, Osaka University, 1-6, Yamadaoka, Suita, Osaka 565-0871, Japan. Tel.: +81 6 6879 8230; fax: +81 6 6879 8234.

E-mail addresses: yasuo@phs.osaka-u.ac.jp (Y. Yoshioka), ytsutsumi@phs.osaka-u.ac.jp (Y. Tsutsumi).

¹ These authors contributed equally to the work.

Co-operation and Development to call for an urgent and detailed evaluation of their safety. Therefore, it is extremely important to progress these safety evaluations in order to facilitate the development of nanomaterials that are harmless to humans, because nanomaterials have the potential to improve the quality of human life. In particular, it is hoped that a risk assessment system can be developed to estimate or predict the safety and toxicity of nanomaterials.

Molecular biomarkers, obtained from biological samples such as blood, urine and tissue, constitute an objective indicator for correlating against various physiological conditions or variation of disease state [13,14]. By using biomarkers, we are able to predict not only the present disease and clinical condition but the risk of acquiring disease in the future. Nowadays, biomarkers that act as predictors of cancer have already been developed and are commonly used in clinical practice [14]. Furthermore, such an approach is capable of predicting adverse effects of drugs and medicines [15,16]. By contrast, studies of biomarkers for nanomaterials have barely advanced. These biomarkers would represent the unity of local and systemic physiological responses induced as a result of the exposure. Therefore, biomarkers for nanomaterials will be invaluable for predicting their potential toxicity and establishing strategies for the safe development of nanomaterials production and use.

Here we attempted to develop potential biomarkers of nanomaterials using a proteomics analysis with the aim of developing safe forms of nanomaterials.

2. Materials and methods

2.1. Materials

Silica particles were purchased from Micromod Partikeltechnologie (Rostock/Warnemünde, Germany). The silica particles with diameters of 30, 70, 300 and 1000 nm (nSP30, nSP70, nSP300 and mSP1000, respectively), and nSP70 with surface functional groups such as carboxyl group and amino group (nSP70-C and nSP70-N, respectively) were used in this study. The silica particles were sonicated for 5 min and vortexed for 1 min prior to use.

2.2. Animals

Female BALB/c mice were purchased from Nippon SLC, Inc (Shizuoka, Japan) and used at 6–8 weeks of age. All of the animal experimental procedures in this study were performed in accordance with the National Institute of Biomedical Innovation guidelines for the welfare of animals.

2.3. Blood sample collection

For administration of silica particles through an intravenous route, BALB/c mice were treated with nSP70, nSP300, mSP1000, nSP70-C, nSP70-N or saline at 0.8 mg/mouse. At various times (6 h, 24 h, 3 day and 7 day) after treatment of these silica particles, blood samples were collected. For administration of silica particles through an intranasal route, BALB/c mice were treated with nSP30, nSP70 or saline intranasally at 0.5 mg/mouse. Blood samples were collected 24 h after the treatment of these silica nanoparticles.

2.4. Analysis of biomarkers for nanomaterials using a proteomics approach

BALB/c mice were treated with 0.8 mg/mouse nSP70 or saline intravenously. After 24 h, blood samples were collected and plasma was harvested by centrifuging blood at 12000 rpm for 15 min. Proteo prep (Sigma–Aldrich; Saint Louis, MO) was used to remove albumin and immunoglobulins from the plasma according to the manufacturer's instructions. Plasma samples were then analyzed by sodium dodecyl sulfate-polyacrylamide gel electrophoresis (SDS-PAGE) followed by Coomassie Brilliant Blue staining. Plasma diluted into aliquots corresponding to 10 µg protein were mixed with an equal volume of Laemmli sample buffer (BIO-RAD, Tokyo, Japan) containing 5% 2-mercaptoethanol and boiled for 5 min prior to electrophoresis. Electrophoresis was performed at 15 mA for 10 min (stacking) followed by separation (600 V, 40 mA, 100 W) for approximately 45 min, using Precision Plus Protein Kaleidoscope molecular weight markers (BIO-RAD) as standards.

2.5. Identification of candidate proteins as biomarkers

Bands of interest were excised from the gel and then destained with 50% acetonitrile (ACN)/25 mM NH_4HCO_3 for 10 min, dehydrated with 100% ACN for 10 min, and then dried using a centrifugal concentrator. Next, 8 µl of 20 µl/ml trypsin solution (Promega, Madison, WI) diluted 5-fold in 50 mM NH_4HCO_3 was added to each gel piece and then incubated overnight at 37 °C. We used three solutions to extract the resulting peptide mixtures from the gel pieces. First, 50 µl of 50% (v/v) ACN in 0.1% aqueous trifluoroacetic acid (TFA) was added to the gel pieces, which were then sonicated for 30 min. Next, we collected the solution and added 80% (v/v) ACN in 0.1% TFA. Finally, 100% ACN was added for the last extraction. The peptide solution were dried and resuspended in 10 µl of 0.1% formic acid. The resulting peptide mixture was then analyzed by nano-flow liquid chromatography/tandem mass spectrometry (LC/MS; maXis, Bruker Daltonik GmbH, Bremen, Germany).

2.6. Measurement of acute phase proteins

Plasma levels of haptoglobin, C-reactive protein (CRP) and serum amyloid A (SAA) were measured by commercial enzyme-linked immunosorbent assay (ELISA) kits (Life Diagnostics, Inc.; West Chester, PA), according to the manufacturer's instructions.

2.7. Statistical analyses

All results are expressed as means \pm SD. Differences were compared by using the Bonferroni's method after analysis of variance (ANOVA).

3. Results

3.1. Identification of biomarkers of nanomaterials

We used silica particles as a model nanomaterial because it is one of the most common nanomaterials to have been developed. Silica particles are increasingly being used as additives in cosmetics and foods [17,18]. It is predicted that the global market for silica particles will soon grow to \$2 billion and a ton of silica particles is currently produced worldwide every year. Here, we used silica particles with a diameter of 30, 70, 300 and 1000 nm (nSP30, nSP70, nSP300 and mSP1000, respectively). The mean secondary particle diameters of the silica particles measured by Zetasizer were 33, 79, 326 and 945 nm, respectively (data not shown). The silica particles were confirmed to be well dispersed smooth-surfaced spheres by transmission electron microscopy (data not shown).

Initially, we attempted to identify protein biomarkers in mice by analyzing changes in the level of each plasma protein following treatment with silica nanoparticles using a proteomics approach. BALB/c mice were intravenously treated with nSP70 (0.8 mg/mouse) or saline and then plasma samples were collected 24 h later. Because albumin and immunoglobulins are known to account for the majority of plasma proteins, they were removed from the samples prior to analysis so that variation in the level of other proteins could be more closely monitored. The change of protein levels in plasma after treatment with nSP70 was assessed by SDS-PAGE analysis (Fig. 1). The intensity of a band of molecular mass 37 kDa was more intense in the plasma of nSP70 treated mice than that of saline treated control mice (Fig. 1). The band was excised and analyzed by LC/MS in order to identify the corresponding protein. This analysis identified the induced band after treatment with nSP70 as haptoglobin, one of the acute phase proteins.

3.2. The level of haptoglobin after treatment with silica particles

To assess the change of haptoglobin level in plasma after administration of silica particles, BALB/c mice were intravenously treated with nSP70, nSP300 or mSP1000 at 0.8 mg/mouse. We did not use nSP30 in the experiment, because nSP30 induced the toxic side effects after intravenous treatment at this dose. We confirmed that nSP70, nSP300 or mSP1000 at this dose did not induce any

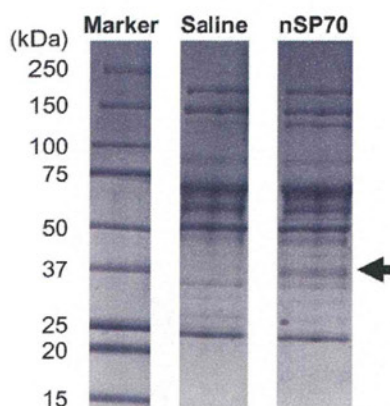


Fig. 1. SDS-PAGE analysis of plasma proteins. BALB/c mice were intravenously treated with nSP70 or saline at 0.8 mg/mouse. After 24 h, blood samples were collected. The change of protein levels in plasma after treatment of nSP70 was assessed by SDS-PAGE.

significant elevation of tissue injury and dysfunction markers such as alanine aminotransferase (ALT), aspartate aminotransferase (AST) and blood urea nitrogen (BUN) (data not shown). After 24 h, the level of haptoglobin in the plasma was analyzed by ELISA (Fig. 2A). The levels of haptoglobin in the plasma of nSP70 treated mice were significantly higher than those of saline treated control mice. In contrast, the levels of haptoglobin in the plasma of mSP1000 treated mice were almost the same as those of the saline treated control group. The haptoglobin levels of nSP300 treated mice were slightly higher than those of saline treated control mice. These results indicate that the levels of haptoglobin in the plasma of mice increase as the silica particle size decreases. Thus, haptoglobin appears to be a valuable biomarker for exposure to silica particles of nanometer size.

To assess the potential of haptoglobin as biomarker more precisely, we examined the sensitivity and time dependency of changes in haptoglobin level after treatment with silica particles. BALB/c mice were treated with nSP70, nSP300 or mSP1000 intravenously at 0.8 mg/mouse. After 6 h, 24 h, 3 day and 7 day, we examined the level of haptoglobin in the plasma by ELISA (Fig. 2B). No elevation of haptoglobin in the plasma of mSP1000 treated mice was observed. However, nSP70 and nSP300 treated mice showed a maximum level of haptoglobin 24 h after treatment. Furthermore, at 3 days after treatment, the level of haptoglobin in nSP70 treated mice was significantly higher than saline treated control mice. Next, BALB/c mice were treated with 0.2 and 0.05 mg/mouse nSP70 intravenously. After 24 h, we examined the level of haptoglobin in the plasma by ELISA (Fig. 2C). Mice treated with 0.2 and 0.05 mg/mouse nSP70 did not show any elevated level of haptoglobin. These results indicate that the level of haptoglobin is elevated as the particle size of silica particles decreases and that an increase of haptoglobin is dependent on the concentration of silica particles.

3.3. Response of other acute phase proteins

Haptoglobin, CRP and SAA are typical acute phase proteins that are induced during infection and inflammation [19]. To assess the levels of CRP and SAA in plasma after administration of silica particles, BALB/c mice were intravenously treated with nSP70, nSP300 or mSP1000 at 0.8 mg/mouse. After 6 h, 24 h, 3 day and 7 day, we examined the level of CRP (Fig. 3A) and SAA (Fig. 3B) in the plasma of the mice by ELISA. At 6 h and 24 h, both the level of CRP and SAA in the plasma of mice treated with nSP70 was significantly higher than those of the saline treated control mice. Furthermore, the maximum level of CRP in nSP70 treated mice was observed at

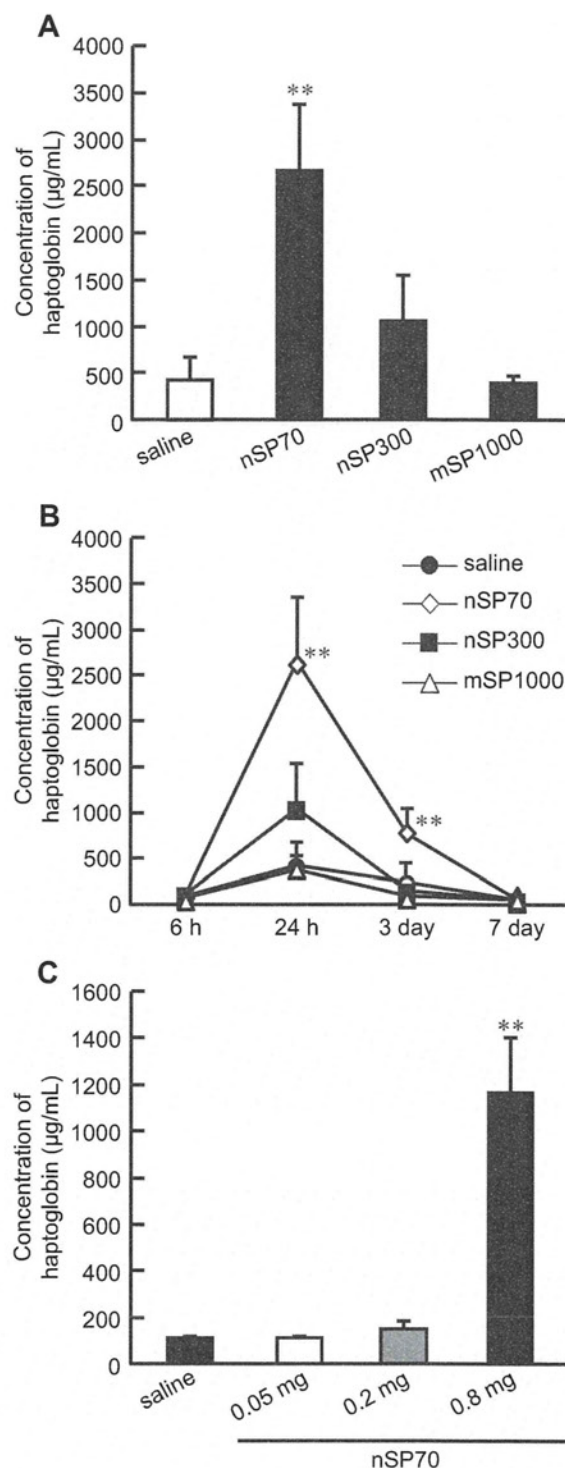


Fig. 2. The potential of haptoglobin as biomarker of nanomaterials. (A) The level of haptoglobin after treatment with silica particles. BALB/c mice were intravenously treated with nSP70, nSP300 or mSP1000 at 0.8 mg/mouse. After 24 h, the level of haptoglobin in the plasma of each mouse was examined by ELISA. (B) The time dependency of haptoglobin expression after treatment with silica particles. BALB/c mice were intravenously treated with nSP70, nSP300 or mSP1000 at 0.8 mg/mouse. After 6 h, 24 h, 3 day and 7 day, blood samples were collected. The level of haptoglobin in the plasma of the mice was determined by ELISA. (C) The sensitivity of haptoglobin after treatment of silica particles. BALB/c mice were intravenously treated with nSP70 at 0.8, 0.2 or 0.05 mg/mouse. After 24 h, blood samples were collected. The level of haptoglobin in the plasma of treated mice was determined by ELISA. Data are presented as mean \pm SD ($n = 5-6$; ** $P < 0.01$ versus value for saline treated group by ANOVA).

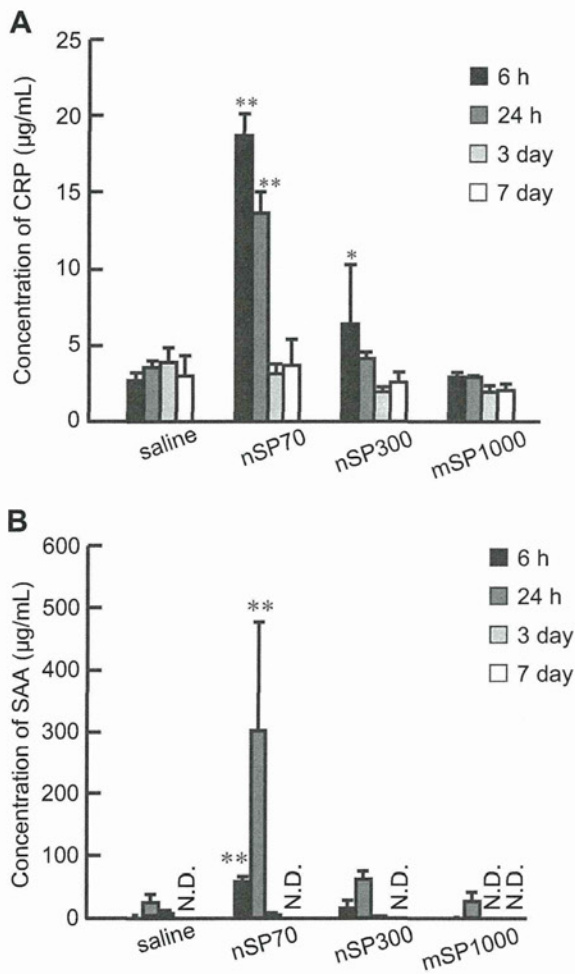


Fig. 3. Response of other acute phase proteins. BALB/c mice were intravenously treated with nSP70, nSP300 or mSP1000 at 0.8 mg/mouse. After 6 h, 24 h, 3 day and 7 day, blood samples were collected. The levels of (A) CRP and (B) SAA in the plasma of treated mice were examined by ELISA. Data are presented as mean \pm SD ($n = 5-6$; * $P < 0.05$, ** $P < 0.01$ versus value for saline treated group by ANOVA; N.D., not detected).

6 h after treatment, whereas that of haptoglobin and SAA was observed at 24 h. In contrast, the level of CRP and SAA in plasma of mSP1000 treated mice were almost the same as that of the saline treated control mice at all time points. The level of CRP in the plasma of nSP300 treated mice was slightly higher than that of saline treated control mice at 6 h. Our results suggest that both SAA and CRP may be useful biomarkers for predicting the risk from exposure to silica nanoparticles as well as haptoglobin. Indeed, these biomarkers could give even better response and sensitivity when used in combination.

3.4. The level of acute phase proteins through various routes

Exposure to nanomaterials in our daily lives can occur through various different routes. For example, nanomaterials contained in foods and drug medicines are taken up orally, whereas nanomaterials spread in the environment generally enter the body intranasally. Therefore, there is a need to evaluate suitable biomarkers for the exposure of nanomaterials through various routes. To assess the response of acute phase proteins to

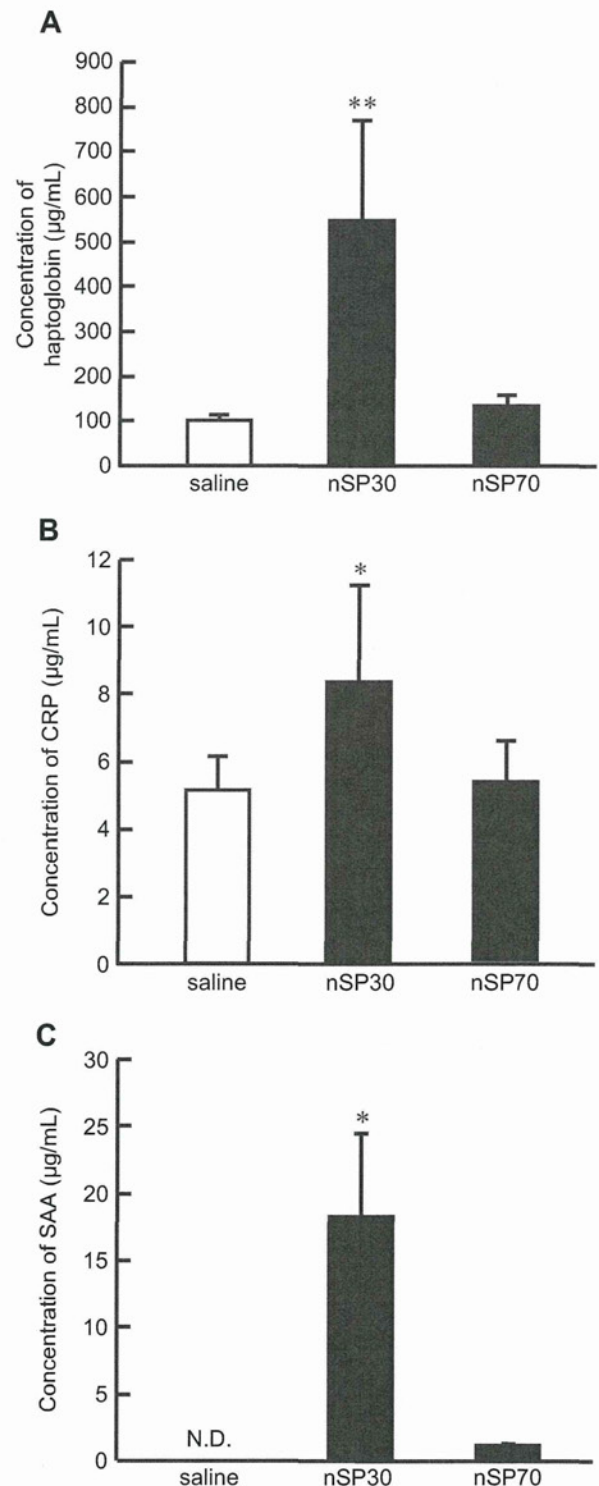


Fig. 4. Application of acute phase proteins to assess exposure of nanomaterials through various routes. To assess the administration of silica nanoparticles through an intranasal route, BALB/c mice were treated with nSP30, nSP70 or saline intranasally at 0.5 mg/mouse. Blood samples were collected 24 h after treatment. The level of (A) haptoglobin, (B) CRP and (C) SAA in the plasma were examined by ELISA. Data are presented as mean \pm SD ($n = 5-6$; * $P < 0.05$, ** $P < 0.01$ versus value for saline treated group by ANOVA; N.D., not detected).

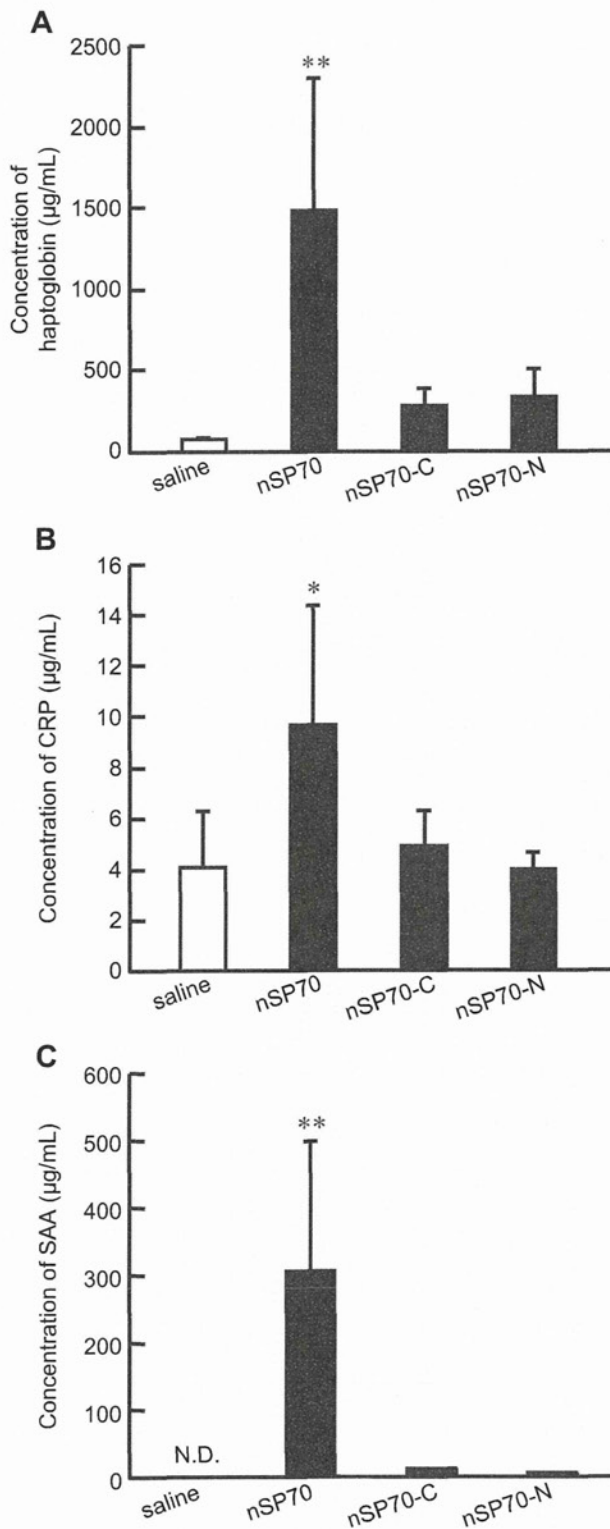


Fig. 5. Responses of acute phase proteins by the exposure to surface modified nSP70. BALB/c mice were intravenously treated with nSP70 modified with amino or carboxyl groups at 0.8 mg/mouse. After 24 h, the level of (A) haptoglobin, (B) CRP and (C) SAA in the plasma of treated mice were examined by ELISA. Data are presented as mean \pm SD ($n = 5-6$; * $P < 0.05$, ** $P < 0.01$ versus value for saline treated group by ANOVA; N.D., not detected).

silica particles introduced via different routes, we examined the level of haptoglobin, CRP and SAA in plasma after treatment of silica particles intranasally (Fig. 4). In this experiment, we used nSP30 and nSP70. For the administration of silica nanoparticles through an intranasal route, BALB/c mice were treated with nSP30, nSP70 or saline intranasally at 0.5 mg/mouse. After 24 h, we examined the level of haptoglobin (Fig. 4A), CRP (Fig. 4B) and SAA (Fig. 4C) in the plasma of the mice by ELISA. We showed that the level of haptoglobin, CRP and SAA in the plasma of mice treated with nSP30 intranasally was significantly higher than those of the saline treated control mice, although intranasal administration of nSP70 did not cause elevation in the plasma level of each acute phase protein in the treated mice. These results suggest that acute phase proteins could be useful biomarkers for predicting the risk arising from exposure to silica nanoparticles through various routes.

3.5. The level of acute phase proteins after treatment with surface modified silica nanoparticles

It has recently become evident that particle characteristics, including particle size and surface properties, are important factors in pathologic alterations and cellular responses [8,20–22]. Previously, our group also showed that surface modification of silica particles with functional groups such as amino or carboxyl group suppressed toxic biological effects of silica particles such as inflammatory responses [23]. To assess whether acute phase proteins could be useful biomarkers to predict risk factors associated with exposure to silica particles, we examined the level of haptoglobin (Fig. 5A), CRP (Fig. 5B) and SAA (Fig. 5C) in the plasma of mice after administration of nSP70 with amino or carboxyl group surface modifications. BALB/c mice were treated with 0.8 mg/mouse of these silica particles intravenously. After 24 h, we examined the level of haptoglobin, CRP and SAA in the plasma of the treated mice by ELISA. Our results showed that the level of these acute phase proteins in the plasma of nSP70 with amino or carboxyl group treated mice were significantly low compared with nSP70 treated mice.

4. Discussion

Our goal was to identify the biomarkers of nanomaterials for predicting their potential toxicity and to provide basic information for the creation of safe nanomaterials. To achieve these purposes, we tried to identify biomarkers in blood using a proteomics analysis. At first, we showed that the silica nanoparticles with small particle sizes (diameter < 100 nm) induced a higher level of acute phase proteins such as haptoglobin, CRP and SAA than larger silica particles (diameter > 100 nm) after intravenously treatment (Figs. 2 and 3). Previously, our group has shown that silica nanoparticles with relatively small particle size such as nSP70 induce a greater level of toxicity, including liver injury, compared to those of larger particle size [10,11]. Thus, there is a correlation between toxicity induced by the silica nanoparticles and the level of each potential plasma biomarker. Therefore, these acute phase proteins appear to be good biomarkers for predicting the strength of toxicity induced by silica nanoparticles.

The acute phase response is the nonspecific early response of an organism to infection and inflammation [24]. It comprises a whole array of systemic reactions and induction of a group of serum proteins called the acute phase proteins [25]. Monitoring the progression of infection and cancer by acute phase protein measurements in blood samples is used extensively in human patients. For example, haptoglobin is a biomarker of pancreatic cancer [26]. CRP is used as an index for the development of atrial fibrillation and maintenance [27], although mouse CRP is

synthesized only in trace amounts unlike its human counterpart [28]. In addition, both SAA and CRP are used as an index for adverse prognosis of breast cancer [29]. Therefore, we believe that these diagnostic systems using acute phase proteins for human health would be useful for predicting the risk of exposure to nanomaterials as well as their likely toxicities. In addition, we showed that the induction time for the maximum level of haptoglobin, SAA and CRP are different after treatment with the silica nanoparticles (Figs. 2 and 3). Therefore, the predictive quality of these biomarkers is improved when they are used in combination.

Epidemiological studies have suggested that increased levels of ambient particle including particle with nanometer size are associated with adverse effects in the respiratory and cardiovascular systems [30]. Some reports have shown that humans exposed to ambient particle have increased blood levels of CRP [31]. In addition, epidemiological studies have shown associations between increased concentrations of SAA and CRP in plasma, and increased risk of cardiovascular diseases [32] and cancer [33]. Therefore we consider that acute phase proteins would be biomarkers for predicting the risk of inflammatory disease, cardiovascular diseases and cancer after exposure by nanomaterials.

In recent years there has been increasing use of nanomaterials in cosmetics, due to their light-diffusing properties and absorbencies, as well as in foodstuffs, such as additives in powdered foods. In particular, silica particles have been extensively used in many consumer products. For example, in the US, the use of amorphous silica is limited to less than 2.0% by weight of common salt. Other limits are defined for finished foods (<1%) and dried egg products (<5%). We cannot avoid exposure to nanomaterials, either from the unintentional release of waste products into the environment or by exposure to medicines, cosmetics and foodstuffs. Thus, it is important to carry out a safety analysis of nanomaterials after exposure via various routes. In this study, we showed that the level of acute phase proteins in the plasma of mice treated with nSP30 intranasally was elevated, although nSP70 did not induce elevation of each acute phase protein (Fig. 4). Therefore we consider that nSP30 would induce any toxic biological effects after intranasally treatment. Now we are trying to examine the pharmacokinetics and biological effects of nSP30 after intranasally treatment.

We then examined the effects of surface modification of silica nanoparticles on the production of acute phase proteins, because it has become evident that surface properties are important factors in the biological effects of particles. We showed that nSP70 with amino or carboxyl group surface modifications did not induce the production of each acute phase proteins (Fig. 5). Previously, we showed that surface modification of silica particles with functional groups such as amino or carboxyl group suppressed toxic biological effects of silica particles such as inflammatory responses [23]. These results also suggest that acute phase proteins could be a promising candidate biomarker for predicting the strength of toxicity induced by silica nanoparticles, although it is need to examine the toxic biological effects of silica nanoparticles with functional groups. Over recent years, nanomaterials have been introduced into our everyday lives. For example, silica particles, titanium dioxide and fullerenes of various crystallographic structures and surface functional groups are used in a range of different consumer products. Therefore, we are now trying to evaluate the response of acute phase proteins to exposure from various nanomaterials.

In general, acute phase proteins are known to be released from the liver mainly as a result of inflammatory cytokines such as interleukin (IL)-6 [19]. However, we confirmed that the levels of IL-6 were not elevated in the plasma of mice treated with silica particles at 24 h after treatment (data not shown). Therefore it is unclear why nanomaterials induce the production of acute phase

proteins. We already showed that although silica particles with micrometer size tend to be taken up by Kupffer cells, silica nanoparticles with small particle sizes distribute around hepatic parenchymal cells (unpublished data). It is conceivable that instead of inflammatory cytokines, small silica particles act directly on the liver to induce the release of acute phase proteins. We are currently analyzing the detailed mechanism by which silica particles induce acute phase proteins in order to identify additional protein biomarkers.

5. Conclusions

We show here that acute phase proteins such as haptoglobin, CRP and SAA can act as useful biomarkers for analyzing the risk of exposure to nanomaterials and their associated toxicity. We believe that such information would be vital for the future development of predictive tests for estimation of the potential toxicity of new nanomaterials based on their physiochemical characteristics.

Acknowledgements

This study was supported in part by Grants-in-Aid for Scientific Research from the Ministry of Education, Culture, Sports, Science and Technology of Japan, and from the Japan Society for the Promotion of Science (JSPS). This study was also supported in part by Health Labour Sciences Research Grants from the Ministry of Health, Labor and Welfare of Japan; by Health Sciences Research Grants for Research on Publicly Essential Drugs and Medical Devices from the Japan Health Sciences Foundation; by a Global Environment Research Fund from Minister of the Environment; and by a the Knowledge Cluster Initiative; and by The Nagai Foundation Tokyo; and by The Cosmetology Research Foundation; and by The Smoking Research Foundation.

References

- [1] Rutherglen C, Burke P. Nanoelectromagnetics: circuit and electromagnetic properties of carbon nanotubes. *Small* 2009;5:884–906.
- [2] Kaur IP, Agrawal R. Nanotechnology: a new paradigm in cosmeceuticals. *Recent Pat Drug Deliv Formul* 2007;1:171–82.
- [3] Cormode DP, Jarzyna PA, Mulder WJ, Fayad ZA. Modified natural nanoparticles as contrast agents for medical imaging. *Adv Drug Deliv Rev* 2010;62:329–38.
- [4] Nel A, Xia T, Madler L, Li N. Toxic potential of materials at the nanolevel. *Science* 2006;311:622–7.
- [5] Donaldson K, Murphy FA, Duffin R, Poland CA. Asbestos, carbon nanotubes and the pleural mesothelium: a review of the hypothesis regarding the role of long fibre retention in the parietal pleura, inflammation and mesothelioma. *Part Fibre Toxicol* 2010;7:5.
- [6] Shvedova AA, Kagan VE, Fadeel B. Close encounters of the small kind: adverse effects of man-made materials interfacing with the nano-cosmos of biological systems. *Annu Rev Pharmacol Toxicol* 2010;50:63–88.
- [7] Poland CA, Duffin R, Kinloch I, Maynard A, Wallace WA, Seaton A, et al. Carbon nanotubes introduced into the abdominal cavity of mice show asbestos-like pathogenicity in a pilot study. *Nat Nanotechnol* 2008;3:423–8.
- [8] Morishige T, Yoshioka Y, Tanabe A, Yao X, Tsunoda S, Tsutsumi Y, et al. Titanium dioxide induces different levels of IL-1beta production dependent on its particle characteristics through caspase-1 activation mediated by reactive oxygen species and cathepsin B. *Biochem Biophys Res Commun* 2010;392:160–5.
- [9] Hougaard KS, Jackson P, Jensen KA, Sloth JJ, Loschner K, Larsen EH, et al. Effects of prenatal exposure to surface-coated nanosized titanium dioxide (UV-Titan). A study in mice. *Part Fibre Toxicol* 2010;7:16.
- [10] Nishimori H, Kondoh M, Isoda K, Tsunoda S, Tsutsumi Y, Yagi K. Silica nanoparticles as hepatotoxicants. *Eur J Pharm Biopharm* 2009;72:496–501.
- [11] Nishimori H, Kondoh M, Isoda K, Tsunoda S, Tsutsumi Y, Yagi K. Histological analysis of 70-nm silica particles-induced chronic toxicity in mice. *Eur J Pharm Biopharm* 2009;72:626–9.
- [12] Nishimori H, Kondoh M, Isoda K, Tsunoda S, Tsutsumi Y, Yagi K. Influence of 70 nm silica particles in mice with cisplatin or paraquat-induced toxicity. *Pharmazie* 2009;64:395–7.
- [13] Casado B, Iadarola P, Luisetti M, Kussmann M. Proteomics-based diagnosis of chronic obstructive pulmonary disease: the hunt for new markers. *Expert Rev Proteomics* 2008;5:693–704.

- [14] Ferte C, Andre F, Soria JC. Molecular circuits of solid tumors: prognostic and predictive tools for bedside use. *Nat Rev Clin Oncol*; 2010 Jun 15 [Epub ahead of print].
- [15] Vaidya VS, Ozer JS, Dieterle F, Collings FB, Ramirez V, Troth S, et al. Kidney injury molecule-1 outperforms traditional biomarkers of kidney injury in preclinical biomarker qualification studies. *Nat Biotechnol* 2010;28:478–85.
- [16] Ozer JS, Dieterle F, Troth S, Perentes E, Cordier A, Verdes P, et al. A panel of urinary biomarkers to monitor reversibility of renal injury and a serum marker with improved potential to assess renal function. *Nat Biotechnol* 2010;28:486–94.
- [17] Villota R, Hawkes JG. Food applications and the toxicological and nutritional implications of amorphous silicon dioxide. *Crit Rev Food Sci Nutr* 1986;23:289–321.
- [18] Merget R, Bauer T, Kupper HU, Philippou S, Bauer HD, Breitstadt R, et al. Health hazards due to the inhalation of amorphous silica. *Arch Toxicol* 2002;75:625–34.
- [19] Gabay C, Kushner I. Acute-phase proteins and other systemic responses to inflammation. *N Engl J Med* 1999;340:448–54.
- [20] He X, Nie H, Wang K, Tan W, Wu X, Zhang P. In vivo study of biodistribution and urinary excretion of surface-modified silica nanoparticles. *Anal Chem* 2008;80:9597–603.
- [21] Nabeshi H, Yoshikawa T, Matsuyama K, Nakazato Y, Arimori A, Isobe M, et al. Size-dependent cytotoxic effects of amorphous silica nanoparticles on Langerhans cells. *Pharmazie* 2010;65:199–201.
- [22] Yamashita K, Yoshioka Y, Higashisaka K, Morishita Y, Yoshida T, Fujimura M, et al. Carbon nanotubes elicit DNA damage and inflammatory response relative to their size and shape. *Inflammation* 2010;33:276–80.
- [23] Morishige T, Yoshioka Y, Inakura H, Tanabe A, Yao X, Narimatsu S, et al. The effect of surface modification of amorphous silica particles on NLRP3 inflammasome mediated IL-1 β production, ROS production and endosomal rupture. *Biomaterials*; 2010 Jun 17 [Epub ahead of print].
- [24] Baumann H, Gauldie J. The acute phase response. *Immunol Today* 1994;15:74–80.
- [25] Kushner I. The phenomenon of the acute phase response. *Ann N Y Acad Sci* 1982;389:39–48.
- [26] Firpo MA, Gay DZ, Granger SR, Scaife CL, DiSario JA, Boucher KM, et al. Improved diagnosis of pancreatic adenocarcinoma using haptoglobin and serum amyloid A in a panel screen. *World J Surg* 2009;33:716–22.
- [27] Korantzopoulos P, Kalantzi K, Siogas K, Goudevenos JA. Long-term prognostic value of baseline C-reactive protein in predicting recurrence of atrial fibrillation after electrical cardioversion. *Pacing Clin Electrophysiol* 2008;31:1272–6.
- [28] Szalai AJ, McCrory MA. Varied biologic functions of C-reactive protein: lessons learned from transgenic mice. *Immunol Res* 2002;26:279–87.
- [29] Pierce BL, Neuhaus ML, Wener MH, Bernstein L, Baumgartner RN, Ballard-Barbash R, et al. Correlates of circulating C-reactive protein and serum amyloid A concentrations in breast cancer survivors. *Breast Cancer Res Treat* 2009;114:155–67.
- [30] Mauderly JL, Chow JC. Health effects of organic aerosols. *Inhal Toxicol* 2008;20:257–88.
- [31] Ruckerl R, Ibald-Mulli A, Koenig W, Schneider A, Woelke G, Cyrys J, et al. Air pollution and markers of inflammation and coagulation in patients with coronary heart disease. *Am J Respir Crit Care Med* 2006;173:432–41.
- [32] Albert MA, Ridker PM. The role of C-reactive protein in cardiovascular disease risk. *Curr Cardiol Rep* 1999;1:99–104.
- [33] Siemes C, Visser LE, Coebergh JW, Splinter TA, Witteman JC, Uitterlinden AG, et al. C-reactive protein levels, variation in the C-reactive protein gene, and cancer risk: the Rotterdam Study. *J Clin Oncol* 2006;24:5216–22.



Systemic distribution, nuclear entry and cytotoxicity of amorphous nanosilica following topical application

Hiromi Nabeshi^{a,b,1}, Tomoaki Yoshikawa^{a,b,1,*}, Keigo Matsuyama^{a,b}, Yasutaro Nakazato^{a,b}, Kazuhiko Matsuo^c, Akihiro Arimori^{a,b}, Masaaki Isobe^{a,b}, Saeko Tochigi^{a,b}, Sayuri Kondoh^{a,b}, Toshiro Hirai^{a,b}, Takanori Akase^{a,b}, Takuya Yamashita^{a,b}, Kohei Yamashita^{a,b}, Tokuyuki Yoshida^{a,b}, Kazuya Nagano^b, Yasuhiro Abe^b, Yasuo Yoshioka^{b,d}, Haruhiko Kamada^{b,d}, Takayoshi Imazawa^e, Norio Itoh^a, Shinsaku Nakagawa^c, Tadanori Mayumi^f, Shin-ichi Tsunoda^{b,g}, Yasuo Tsutsumi^{a,b,d,*}

^a Department of Toxicology and Safety Science, Graduate School of Pharmaceutical Sciences, Osaka University, 1-6 Yamadaoka, Suita, Osaka 565-0871, Japan

^b Laboratory of Biopharmaceutical Research (Pharmaceutical Proteomics), National Institute of Biomedical Innovation, 7-6-8 Saito-Asagi, Ibaraki, Osaka 567-0085, Japan

^c Department of Biotechnology and Therapeutics, Graduate School of Pharmaceutical Sciences, Osaka University, 1-6 Yamadaoka, Suita, Osaka 565-0871, Japan

^d The Center for Advanced Medical Engineering and Informatics, Osaka University, 1-6 Yamadaoka, Suita, Osaka 565-0871, Japan

^e Bioresources Research, Laboratory of Common Apparatus, National Institute of Biomedical Innovation, 7-6-8 Saito-Asagi, Ibaraki, Osaka 567-0085, Japan

^f Graduate School of Pharmaceutical Sciences, Kobe-Gakuin University, 1-1-3 Minatogima, Chuo-ku, Kobe, Hyogo 650-8586, Japan

^g Department of Biomedical Innovation, Graduate School of Pharmaceutical Sciences, Osaka University, 7-6-8 Saito-Asagi, Ibaraki, Osaka 567-0085, Japan

ARTICLE INFO

Article history:

Received 12 October 2010

Accepted 27 December 2010

Available online 22 January 2011

Keywords:

Nanoparticles

Silica

Transdermal penetration

Cytotoxicity

Mutagenicity

ABSTRACT

Currently, nanomaterials (NMs) with particle sizes below 100 nm have been successfully employed in various industrial applications in medicine, cosmetics and foods. On the other hand, NMs can also be problematic in terms of eliciting a toxicological effect by their small size. However, biological and/or cellular responses to NMs are often inconsistent and even contradictory. In addition, relationships among NMs physicochemical properties, absorbency, localization and biological responses are not yet well understood. In order to open new frontiers in medical, cosmetics and foods fields by the safer NMs, it is necessary to collect the information of the detailed properties of NMs and then, build the prediction system of NMs safety. The present study was designed to examine the skin penetration, cellular localization, and cytotoxic effects of the well-dispersed amorphous silica particles of diameters ranging from 70 nm to 1000 nm. Our results suggested that the well-dispersed amorphous nanosilica of particle size 70 nm (nSP70) penetrated the skin barrier and caused systemic exposure in mouse, and induced mutagenic activity *in vitro*. Our information indicated that further studies of relation between physicochemical properties and biological responses are needed for the development and the safer form of NMs.

© 2011 Elsevier Ltd. All rights reserved.

1. Introduction

A nanomaterial (NM) is defined as a substance that has at least one dimension of less than 100 nm in size. NMs can assume many different forms, such as tubes, rods, wires, spheres or particles. NMs have been widely used in consumer and industrial applications, such as medicine, cosmetics and foods, because they exhibit unique physicochemical properties and innovative functions [1]. However,

NMs can also be problematic in terms of eliciting a toxicological effect by their small size. For example, exposure of cells or animals to carbon nanotubes, titanium dioxide nanoparticles or silver nanoparticles can induce cytotoxicity and inflammation [2–14]. We have previously shown that nSPs display a different intracellular localization compared with submicron- and micro-sized silica particles, and induce a greater cytotoxic response [15]. Whereas other studies reported that carbon nanotubes and titanium dioxide nanoparticles do not induce harmful effects [16–18]. Thus, despite intensive research efforts, reports of biological and/or cellular responses to NMs are often inconsistent and even contradictory. In addition, relationships among NMs physicochemical properties, absorbency, localization and biological responses are not yet well understood. In order to ensure the safety of NMs and open new frontiers in biological fields by the use of NMs, it is necessary to

* Corresponding authors. Department of Toxicology and Safety science, Graduate School of Pharmaceutical Sciences, Osaka University, 1-6 Yamadaoka, Suita, Osaka 565-0871, Japan. Tel.: +81 6 6879 8230; fax: +81 6 6879 8234.

E-mail addresses: tomoaki@phs.osaka-u.ac.jp (T. Yoshikawa), ytsutsumi@phs.osaka-u.ac.jp (Y. Tsutsumi).

¹ These authors contributed equally to the work.

collect the information of the detailed properties of NMs from the point of view of biosafety and then, build comprehensive prediction system of NMs safety.

Accordingly, in this study, we evaluated the absorption properties and intracellular distribution of NMs, using typical NMs, amorphous nanosilica particles (nSP) and quantum dots (QD). nSP are one of the most widely applied NMs, and are used in cosmetics and food additives. nSPs and QD also have great potential for use as diagnostic imaging agents, gene delivery carriers and cancer therapies [19–23]; in addition, these NMs show overwhelmingly superior dispersibility as compared with carbon nanotubes, fullerene and nano-sized titanium dioxide (TiO₂). Thus, these NMs are ideally suited for determining how particle size influences the biodistribution and biological effects of NMs.

2. Materials and methods

2.1. Silica particles

Suspensions of fluorescent (red-F)-labeled amorphous silica particles (Micro-mod Partikeltechnologie GmbH) (25 mg/ml and 50 mg/ml) were used in this study; particle size diameters were 70, 300 and 1000 nm (designated as nSP70, nSP300 and mSP1000, respectively). Silica particles were used following 5 min sonication and 1 min vortex.

2.2. Quantum dots

Quantum dots (QD) with emission maxima at 565 nm were obtained from Invitrogen (Hayward, CA). They were sold as Qtracker[®] Non-targeted Quantum Dots (PEG). QD were used after 5 min sonication and 1 min vortex.

2.3. Animals

BALB/c mice (female, 6–8 weeks) were purchased from Japan SLC, Inc. Mice were housed in a ventilated animal room maintained at 20 ± 2 °C with a 12-h light/12-h dark cycle. Mice had free access to water and alfalfa-free forage (FR-2, Funabashi farm). The experimental protocols conformed to the ethical guidelines of the National Institute of Biomedical Innovation.

2.4. Cell culture

HaCaT human keratinocyte cell line was kindly provided by Dr. Inui, Osaka University. HaCaT cells were cultured in Dulbecco's modified Eagle's medium (D-MEM) supplemented with 10% heat-inactivated fetal bovine serum and 0.2 mM L-glutamine. The cells were grown in a humidified incubator at 37 °C (95% room air, 5% CO₂).

2.5. Physicochemical examinations of silica particles and QD

Silica particles and QD were diluted to 0.25 mg/ml (nSP70), 0.5 mg/ml (nSP300 and mSP1000) or 0.5 μM (QD) with PBS, respectively and the average particle size and zeta potential were measured using the Zetasizer Nano-ZS (Malvern Instruments Ltd). The mean size and the size distribution of silica particles were measured by dynamic light scattering method. The zeta potential was measured by laser Doppler electrophoresis. pH of each particles suspension were measured by ISFET-pH meter (SHINDENGEN, Japan). The size and shape of silica particles and QD were observed using transmission electron microscopy (TEM). Prior to TEM analysis, nSP70 were stained with 2% uranium acetate and QD were enhanced by silver using a standard AURION R-GENT SE-EM reagent and protocol.

2.6. Dermal administration of silica particles and transmission electron microscopy (TEM) analysis of skin, lymph node and liver

nSP70 (250 μg/ear/day) and QD (1.2 pmol/ear/day) suspension supplemented with 10% isopropyl myristate were applied to the inner side of both ears of BALB/c mice for 28 days. In both samples, the total number of particles applied over 28 days was 2.8 × 10¹³ particles. After 24 h of last administration, skin, lymph node and brain from each mouse were excised and fixed in 2.5% glutaraldehyde for 2 h. Then, small pieces of tissue sample were washed with phosphate buffer three times and post-fixed in sodium cacodylate-buffered 1.5% osmium tetroxide for 60 min at 4 °C, block stained in 0.5% uranyl acetate, dehydrated by dipping each of them through a series of ethanol solutions containing increasing concentration of ethanol, and embedded in Epon resin (TAAB). Ultrathin sections were stained with uranyl acetate and lead citrate (silica particles-treated samples) or AURION R-GENT SE-EM reagent (QD-treated samples). The stained samples were subsequently observed under a Hitachi electron microscope (H-7650).

2.7. Detection of apoptotic cells in the nSP70-applied mice skin (terminal deoxynucleotidyl transferase-mediated X-dUTP nick-end labeling (TUNEL) staining)

The TUNEL staining was performed on paraffin-embedded skin sections of 28-day application of nSP70. The skin was fixed in 10% neutral buffered formalin and then embedded in paraffin. Paraffin-embedded skin was sliced and placed on glass slides. DNA strand breaks, which are associated with the apoptotic response, were detected with an *in situ* Cell Death Detection Kit, TMR red (Roche) according to protocol of this kit. Deparaffinization and rehydration of the skin sections were carried out according to standard protocols. Then, the skin sections were incubated with proteinase K for 30 min. After rinse of the skin sections twice with PBS, 50 μl of TUNEL reaction mixture were added on the skin sections and incubated for 60 min at 37 °C in the dark. The skin sections were rinsed 3 times with PBS and mounted with the mounting agent, ProLong Gold Antifade Reagent with DAPI (Invitrogen). The skin sections were analyzed under a fluorescence microscope (BIOREVO, KEYENCE) with excitation wavelength in the range of 520–560 nm and detection in the range of 570–620 nm. For counting the numbers of TUNEL-positive cells, approximately 1000 cells were randomly selected from 3 different areas in each section and examined under a fluorescence microscope at magnification of ×200.

2.8. Transmission electron microscopy (TEM) analysis of human keratinocyte cells

HaCaT cells were cultured in the presence of various sized silica particles (100 μg/ml) for 24 h on chamber slides, and then fixed in 2.5% glutaraldehyde followed by 1.5% osmium tetroxide. The fixed cells were dehydrated and embedded in EPON resin. Ultrathin sections were stained with lead citrate and observed under an electron microscope.

2.9. Evaluation of the proliferation of silica particle- or QD-treated cells (³H-thymidine incorporation assay)

Proliferation of silica particle- or QD-treated HaCaT cells was measured by ³H-thymidine incorporation assay. 1 × 10⁴ cells were cultured with varying concentrations of silica particles or QDs for 18 h at 37 °C and ³H-thymidine (1 μCi/well) was then added into each well. After a further 6 h, cells were harvested and lysed on glass fiber filter plates using a Cell harvester (PerkinElmer). The filter plates were then dried and counted by standard liquid scintillation counting techniques in a Top-Counter (PerkinElmer).

2.10. Mutagenicity assay (Ames test)

The mutagenicity assay was performed to evaluate the intrinsic mutagenic potency of the silica particles. For this purpose, the *Salmonella typhimurium* (*S. typhimurium*) mutagenicity test was performed according to the method of Ames [24–26]. Two strains of *S. typhimurium* bacteria were used, namely, TA98 and TA100. Experiments were conducted according to guideline of Health, Labour and Welfare Ministry. The test was carried out using 100 μl of well-dispersed solutions (10, 90, and 810 μg/ml) of silica particles. 2-Aminofluorene (2-AF) dissolved in DMSO was used as a positive control for the mutagenicity assay.

2.11. Determination of DNA damage (comet assay)

Damage of endogenous DNA in HaCaT cells after treatment with a given silica particles were analyzed by alkaline comet assay according to the Comet Assay Kit (Trevigen). All steps were conducted under dim yellow light to prevent additional DNA damage. Briefly, 3 × 10⁴ HaCaT cells were seeded into each well of a 6-well plate and incubated for 24 h. After 24 h, cells were treated with 30 or 90 μg/ml nSP70, nSP300, mSP1000 or 0.2 mM H₂O₂ (positive control) or PBS (negative control) for 3 h. Cells from each group were resuspended at a density of 1 × 10⁵ cells/ml in ice cold CMF-PBS and combined with molten LM Agarose (Trevigen) at a ratio of 1:10 (v/v). The cell-agarose mixture was immediately pipetted onto a frosted microscope slide (CometSlide; Trevigen). Each slide was then placed flat at 4 °C in the dark for 60 min, immersed in prechilled lysis solution (Trevigen), and left at 4 °C for 40 min to remove cellular proteins, leaving the DNA molecules exposed. The slides were then immersed in an alkaline solution (pH > 13, 0.3 M NaOH and 1 mM EDTA) for 40 min to denature the DNA and hydrolyze the sites that were damaged. The samples were electrophoresed for 10 min and stained with SYBR green I (Trevigen) according to the manufacturers instructions. Twenty-five cells on each slide, randomly selected by fluorescence microscopy, were then analyzed using the Comet Analyzer (Youworks Corporation).

2.12. In vivo imaging

Biodistribution of fluorescent-labeled silica particles was analyzed in live mice and excised tissues using the IVIS 200 imaging system (Xenogen corp.). Three female Hos: HR-1 mice were treated with 100 mg/kg DY-676 (excitation (ex) and emission (em) wavelengths 674 and 699 nm, respectively)-labeled silica particles of each particle size (70, 300 and 1000 nm) by intravenous injection. After anesthesia with isoflurane, live mouse fluorescence optical imaging was performed using the cy5.5

filter set (ex/em 615–665/695–770). Tissues were then excised from the mice and fluorescent images of the tissues were obtained. Imaging parameters were selected and implemented using the instrument, Living Image 2.5 software. Bright field photographs were obtained for each imaging time. The merged bright field photographs and fluorescent images were generated using Living Image 2.5 software.

2.13. Transmission electron microscopy (TEM) analysis of liver

BALB/c mice were treated with 0.6 mg/mouse (about 30 mg/kg, 70 nm) or 2 mg/mouse (about 100 mg/kg, 300 and 1000 nm) silica particles of each particle size and PBS (control) by intravenous injection. After 24 h, the tissues and organs such as brain, heart, lung, liver, kidney, spleen and lymph node, were excised and fixed in 2.5% glutaraldehyde for 2 h. Small pieces of tissue sample were then washed with phosphate buffer three times and postfixed in sodium cacodylate-buffered 1.5% osmium tetroxide for 60 min at 4 °C, block stained in 0.5% uranyl acetate, dehydrated through a series of ethanol concentrations, and embedded in Epon resin (TAAB). Ultrathin sections were stained with uranyl acetate and lead citrate. The samples were examined under a Hitachi electron microscope (H-7650).

2.14. Living cell counting and DNA damage determination in isolated primary hepatocytes from silica particle-treated mice

Female BALB/c mice were treated with 2 mg/mouse (about 100 mg/kg) silica particles of each particle size (70, 100, 300 and 1000 nm) and PBS (control) by intravenous injection. After 5 h, parenchymal hepatocytes were isolated according to the *in situ* two-step collagenase perfusion technique. Briefly, the liver was perfused with 25 ml of 10 mM Hepes buffered calcium- and magnesium-free Hanks' balanced salt solution (HBSS) containing 190 mg/l EGTA (DOJINDO) for 5 min. The liver was then perfused with 40 ml of HBSS containing 250 mg/l trypsin inhibitor, 500 mg/l collagenase and 550 mg/l CaCl₂ for 10 min. The liver was then excised and the cells dispersed in HBSS. The cells were then centrifuged at 50 × g at 4 °C for 1 min. The resulting pellet was resuspended in 20 ml of L15 medium containing 5% FCS, 1 μM dexamethasone and 1 μM insulin and centrifuged at 50 × g at 4 °C for 1 min. This step was repeated 3 times. The resulting pellet was resuspended in medium and living cells were counted using trypan blue staining. Endogenous DNA damage in isolated primary parenchymal hepatocytes from mice treated with nSP70, nSP300, mSP1000 and PBS (control) was analyzed by alkaline comet assay as described above.

2.15. Statistical analysis

Statistical comparisons between groups were performed by one-way ANOVA with Bonferroni test as a *post hoc* test. The level of significance was set at $P < 0.05$.

3. Results and discussion

3.1. Physicochemical properties of various sized silica particles and QD

The first step for ensuring the biosafety of NMs are to evaluate whether the NMs could penetrate the epithelial barriers, could eventually become absorbed systemically, and more importantly, whether they could be responsible for acute/chronic side effects. In this context, here, we evaluated whether the nSP and QD could penetrate into the skin of BALB/c mice following dermal exposure. Prior to undertaking the skin penetration study, we first analyzed the physicochemical properties of the commercially available silica particles of 70, 300 and 1000 nm in diameter (nSP70, nSP300 and mSP1000, respectively). Close examination of the silica particles of different particle sizes by TEM revealed that all silica particles used in this study were smooth-surfaced spherical particles and in size category the primary particle sizes were approximately uniform (Fig. 1a–f). According to technical datasheet, surface textures of all silica particles were plain and nonporous. The specific surface area was calculated by means of the following equation; $s = 6/d\rho$ (where s , specific surface area (m²/g); ρ , density (g/cc); d , diameter (μm)). The specific surface area of nSP70, nSP300 and mSP1000 calculated using this equation was 43, 10 and 3 m²/g, respectively. In addition, all silica particles used in this study was not modified with any functional groups. These physicochemical properties were summarized in Table 1. From the results of mean particle size in solution, it was suggested that the silica particles used in this study remained as stable well-dispersed particles in solution, and not as aggregates.

Thus, these particles are ideally suited as optimal sample to evaluate if and whether their biodistribution and biological effect depend on the particle size. As well as silica particles, the shape, size distribution and zeta potential of QD were evaluated. Surface of QD used in this study were coated with polyethylene glycol (PEG). QD were enhanced using silver for TEM analysis, because silver selectively deposits on the QD [27]. From the results of TEM analysis, QD were also spherical particles, and in terms of size category the primary particle sizes (about 35 nm) were approximately uniform. The size distribution spectrum of QD in a neutral solvent showed two peaks, and the average particle size of peaks 1 and 2 was about 35 and 300 nm, respectively.

3.2. Analysis of transdermal penetration and biodistribution of nanosilica and QD applied on the skin

We next used TEM to determine whether nSP with a particle size below 100 nm would penetrate the skin after topical application. As a result, the 28-day application of nSP70 to mice showed that nSP70 entered not only the skin (Fig. 2a), the regional lymph nodes (Fig. 2b) and the parenchymal hepatocytes present in liver (Fig. 2c, d) but also the cerebral cortex (Fig. 2e) and the hippocampus (Fig. 2f). Surprisingly, penetration of nSP70 into the liver was also detected, and some of the nSP70 that entered the parenchymal hepatocytes were found to be distributed throughout the cytoplasm and inside the nucleus (Fig. 2c) and mitochondria (Fig. 2d). Localization of nSP70 in the nucleus was also detected in the skin and the lymph node (Fig. 2a, b). Next, the skin permeability of QD was evaluated. We found that QD penetrated the stratum corneum and entered the skin (Fig. 2g), lymph node (Fig. 2h), liver (Fig. 2i, j), cerebral cortex (Fig. 2k) and hippocampus (Fig. 2l). In addition, some of the QD that entered the skin (Fig. 2g), lymph node (Fig. 2h) and parenchymal hepatocytes (Fig. 2i) were detected inside the nucleus, similar to nSP70. We considered that the well-dispersed portion of QD showed skin permeability. It has been reported that QD can enter the skin by transdermal exposure under ultraviolet radiation [27]. However, for the first time we have revealed that nSP and QD penetrate the skin and enter tissues such as the lymph node, liver and brain under normal conditions.

3.3. Analysis of biological effects induced by nanosilica and QD

The next step for the biosafety should include analyzing their biological effects against skin, brain, liver and lymph node. Consequently, first, in order to assess the biological response in the skin as a part of 28-day application of nSP70, we tried to detect the apoptotic cells by using Terminal Deoxynucleotidyl Transferase-Mediated X-dUTP Nick-End Labeling (TUNEL) staining. As a result, while a few TUNEL-positive cells were detected in water-applied mice skin (control) (Fig. 3a), a number of TUNEL-positive cells (expressed in red) were detected in nSP70-applied mice skin (Fig. 3b). The ratio of TUNEL-positive cells in the skin sections of mice transdermally-applied with nSP70 tended to increase compared to mice transdermally-applied with water (control). In one of two nSP70-applied mice, the ratio of TUNEL-positive cells in the skin section was dominantly increased (Fig. 3c). This result suggested that the transdermal application of nSP70 induced the cellular damage in the skin. On the basis of this result and transdermal absorption test results, we are now evaluating higher cerebral function, hepatic drug metabolism, and the immune system of mice after topical nSP exposure. Moreover, it is necessary to evaluate the influence of well-dispersed NMs on nuclear and mitochondrial functions, because we found that nSP70 and QD enter into these specific organelles. These results also suggest that systemic safety analysis (hazard analysis) of an NM is highly important for ensuring its safety. Because nSP70 and QD can

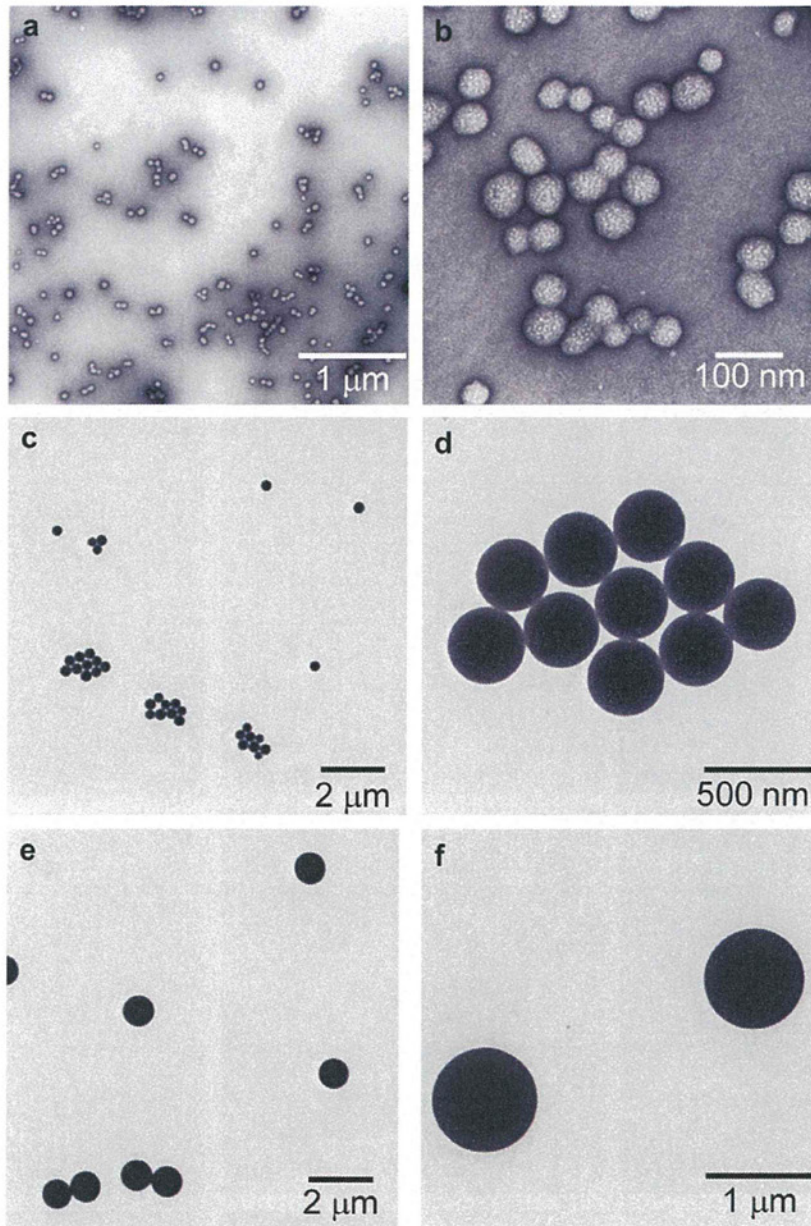


Fig. 1. Transmission electron microscopy (TEM) analysis of silica particles. a–f, TEM photomicrographs of silica particles used in this study: nSP70 (a and b), nSP300 (c and d) and mSP1000 (e and f). Each type of sized silica particles existed as scattered and spheroidal. Scale bars: 1 μm (a and f), 100 nm (b), 500 nm (d) and 2 μm (c and e).

penetrate the skin barrier, which is the most rigid biological barrier, we believe that analysis of oral and pulmonary exposure should also be included in ensuring the biosafety of NMs.

Collectively, these observations clearly show that nSPs and QD of less than 100 nm in diameter invade the body through the skin,

suggesting that human beings are at high risk of exposure to NMs through the blood stream. Consequently, we analyzed the distribution and biological effects of NMs with a focus on the region level and the systemic level. Because nSPs have already been put into practical use in cosmetics, firstly, we evaluated the intracellular

Table 1
Summary of the physicochemical properties of silica particles.

	Primary particle size (nm) ^a	Hydrodynamic diameter (nm)	Mean zeta potential (mV)	pH	Surface texture ^a	Porosity ^a	Surface area (m^2/g) ^b	Functional group ^a
nSP70	70	77.0 ± 0.4	-21.6 ± 4.5	7.4	Plain	Nonporous	43	None
nSP300	300	269.3 ± 2.1	-31.3 ± 6.5	7.5	Plain	Nonporous	10	None
mSP1000	1000	1187 ± 25.2	-37.7 ± 4.6	7.9	Plain	Nonporous	3	None

Mean particle size and zeta potential in solution of silica particles are expressed as mean \pm S.D. ($n = 3$).

^a Information from technical datasheet of products.

^b The specific surface area was calculated by means of the following equation; $s = 6/d\rho$ (where s , specific surface area (m^2/g); ρ , density (g/cc); d , diameter (μm)).